

A Communication-Bandwidth-Aware Hybrid Estimation Framework for Multi-robot Cooperative Localization

Esha D. Nerurkar and Stergios I. Roumeliotis

Abstract—This paper presents hybrid Minimum Mean Squared Error-based estimators for wireless sensor networks with *time-varying* communication-bandwidth constraints, focusing on the particular application of multi-robot Cooperative Localization. When sensor nodes (e.g., robots) communicate only a quantized version of their analog measurements to the team, our proposed hybrid filters enable robots to process all available information, i.e., local analog measurements (recorded by its *own* sensors) as well as remote quantized measurements (collected and communicated by *other* sensors). Moreover, these filters are *resource-aware* and can utilize additional bandwidth, whenever available, to maximize estimation accuracy. Specifically, in this paper, we present two filters, the Hybrid Batch-Quantized Kalman filter (H-BQKF) and the Hybrid Iteratively-Quantized Kalman filter (H-IQKF), that can process local analog measurements along with remote measurements quantized to *any number of bits*. We test our proposed filters in simulations and experimentally, and demonstrate that they achieve performance comparable to the standard Kalman filter.

I. INTRODUCTION AND RELATED WORK

In wireless sensor (robot) network (WSN) applications (e.g., target tracking and environmental monitoring), sensors typically estimate a quantity of interest, using noisy measurements from *all* sensor nodes. Since the sensor nodes are spatially distributed, each node generally has to communicate its local information to the team, either as estimate-covariance pairs or as raw measurements [1], incurring substantial communication overhead. Therefore, for WSNs deployed in (i) environments with inherent communication limitations or (ii) applications with power/battery restrictions, it becomes necessary to develop decentralized estimation algorithms that can trade communication bandwidth-availability for estimation accuracy. While bandwidth constraints exist in many WSN applications, this work focuses on the representative application of Cooperative Localization (CL).

In GPS-denied environments (e.g., space or indoors), CL is used for accurate multi-robot localization, i.e., precisely estimating the robots' poses (position and orientation). In CL, communicating robots equipped with proprioceptive (e.g., wheel encoders) and exteroceptive (e.g., cameras) sensors use their individual motion measurements (e.g., linear/rotational velocity) and robot-to-robot relative measurements (e.g., distance/bearing) to *jointly* estimate their poses, resulting in increased accuracy for the entire team [2].

This work was supported by the University of Minnesota (DTC), and the National Science Foundation (IIS-0643680). E. D. Nerurkar was supported by the UMN Doctoral Dissertation Fellowship.

E. D. Nerurkar, and S. I. Roumeliotis are with the Department of Computer Science and Engineering, Univ. of Minnesota, Minneapolis, USA {nerurkar, stergios}@cs.umn.edu

Representative works for bandwidth-constrained CL include the extended Kalman filter (EKF)-based approaches of [3], [4], and [5], where based on a suitable selection/optimality criterion, the robots select and transmit their most informative analog measurements¹. Similarly, Maximum A Posterior (MAP) estimator-based approaches for CL, where the robots only periodically exchange local information, are presented in [6], [7]. However, in contrast to these approaches, which assume that robots can communicate all or a subset of their analog measurements, the work presented in this paper focuses on applications with stringent communication bandwidth constraints, where robots can communicate *only a few bits per analog measurement*. Therefore, each robot has to perform *lossy quantization* of its analog measurements before communicating them to the team. Moreover, the existing estimators such as the EKF and MAP, designed for processing *only* analog measurements, have to be modified to handle the quantized measurements.

Estimation with quantized observations has been well-studied in the signal processing community for WSNs. While there exists a large body of work on parameter estimation (either deterministic [8], [9], [10] or random variable [11], [12], [13]), we will focus on approaches that were developed to estimate random processes, as is the case in CL. The Sign-of-Innovation Kalman filter (SOI-KF) [14], has been proposed for estimating stochastic dynamic processes, where the measurement innovation², instead of the actual analog measurement, is quantized to a single bit. Developed for linear and Gaussian process and measurement models, the SOI-KF approximates the posterior probability density function (pdf) by a Gaussian³ after each measurement update, resulting in a recursive state/covariance update structure very similar to that of the standard Kalman filter [15]. When additional bits are available for quantization, the SOI-KF approach has been extended in [16] to the batch-quantized KF (BQKF) and the iteratively-quantized KF (IQKF), where performance comparable to the standard KF can be achieved by communicating only 4 bits per analog measurement. An extension to quantized batch MAP estimation, that improves estimation accuracy when using nonlinear process and measurement models, is presented in [17].

¹Sensors sample a process and provide a measurement which is often represented in digital form using 32 or 64 bit floating-point number representation. We refer to such measurements as analog.

²Measurement innovation is the difference between the actual and the estimated (by the filter) measurement.

³Note that due to the nonlinearity of the quantization operation, the posterior pdf is not, in general, a Gaussian.

The main drawback of these quantized estimation schemes, however, is that they prohibit the robots from utilizing all locally-available measurement information. Specifically, to ensure estimation consistency, each robot is compelled to use only quantized versions of its *own* local, analog measurements. Thus, valuable information, that can be used to improve localization accuracy, is discarded.

In [18], we introduced a hybrid estimation framework that addresses this problem by maintaining two local estimators for each robot (see Fig. 1): (i) a quantized Q-estimator processing quantized measurements from all robots, including itself, and (ii) a hybrid H-estimator processing its own analog measurements along with the quantized measurements from other robots in the team. The H-estimator in [18] is designed for the special/restrictive scenario when robots communicate *only a single bit* per analog measurement.

In practice, however, the communication bandwidth available for CL is often *time-varying*, and depends upon the resource requirements of higher-level tasks and the robots' battery life. Therefore, in this work, our objective is to efficiently utilize additional bandwidth, whenever available, to maximize localization accuracy. To achieve this, in this paper, we derive H-estimators that can handle the *general* case of *time-varying* communication-bandwidth availability, i.e., when robots in the team can communicate $f \geq 1$ bits, per analog measurement. Specifically, we develop H-estimators (see Section III) for two quantization scenarios: (i) Batch quantization: where the bandwidth availability is known beforehand, and (ii) Iterative quantization: where additional bandwidth becomes available on-the-fly. For both these scenarios, we derive Minimum Mean Squared Error-based (MMSE) H-estimators (H-BQKF and H-IQKF, respectively) that are capable of processing local analog measurements along with multiple bits per remote analog measurement. Lastly, in Section IV, we present extensive simulation and experimental results that study the performance and accuracy of the proposed H-estimators.

II. PROBLEM FORMULATION

The proposed hybrid MMSE-based estimators are designed for WSNs where (i) the process and measurement models are shared *a priori* by all sensor nodes, and (ii) each sensor node can communicate with the network at every time step. While we now proceed with the specific application of CL, we note that the proposed estimators are general and can be used for any static/mobile sensor network applications that satisfy the above assumptions.

For CL, the problem setup consists of a team of N robots performing multi-centralized CL (MC-CL) in 2D. In MC-CL, each robot broadcasts *all* its measurements and every robot locally processes measurements from the entire team to estimate the robots' joint state. The robot team uses a statistical motion model (e.g., constant-velocity model [19]), driven by system noise, as the process model:

$$\mathbf{x}_k = \mathbf{F}_{k-1}\mathbf{x}_{k-1} + \mathbf{G}_{k-1}\mathbf{w}_{k-1}, \quad \mathbf{x}_0 \sim \mathcal{N}(\mathbf{x}_{init}, \mathbf{P}_0) \quad (1)$$

where, \mathbf{w}_k is the zero-mean, white, Gaussian, and uncorrelated system noise at time-step k with covariance $E[\mathbf{w}_k\mathbf{w}_k^T] = \delta_{kl}\mathbf{Q}_k$. Here, $\mathbf{x}_k = [\mathbf{x}_k^1, \mathbf{x}_k^2, \dots, \mathbf{x}_k^N]^T$, is the joint-state of the team and $\mathbf{x}_k^i = [x_k^i, y_k^i, \phi_k^i]^T$, is the state (position and orientation) of robot i at time-step k .

Robot i obtains M_k^i scalar, analog measurements (proprioceptive and exteroceptive) at time-step k . The measurement model for robot i , $i = 1, \dots, N$, is:

$$z_{km}^i = \mathbf{h}_{km}^{iT}\mathbf{x}_k + v_{km}^i, \quad m = 1, \dots, M_k^i \quad (2)$$

where v_{km}^i is zero-mean, white, Gaussian, and uncorrelated measurement noise with $E[v_{km}^i v_{ln}^i] = \delta_{kl, mn}\sigma_{km}^2$ and $E[v_{km}^i v_{ln}^j] = 0$, $\forall j \neq i$, $j = 1, \dots, N$. Here, the linear models (1)-(2) are used only for mathematical derivations. In real-world scenarios with nonlinear models (see Section IV), the corresponding *linearized* system models are used. Also, to simplify the notation in the paper, we will assume that each robot i obtains only a single, scalar, analog measurement, z_k^i , at time-step k . The generalization to M_k^i measurements is straightforward.

In the absence of communication-bandwidth constraints, the robots broadcast their analog measurements to the team. Then each robot uses the standard KF [15] to obtain the Minimum Mean Squared Error (MMSE) estimates of all robots' poses at time-step k , given *all analog* measurements, $\mathbf{z}_{0:k}$, up to time-step k . Here, $\mathbf{z}_{0:k} = [(\mathbf{z}_{0:k}^1)^T, \dots, (\mathbf{z}_{0:k}^N)^T]^T$ and $\mathbf{z}_{0:k}^i = [z_0^i, \dots, z_k^i]^T$, $i = 1, \dots, N$. On the contrary, in the bandwidth-limited scenario, each robot can communicate only $f \geq 1$ bits per analog measurement. Therefore, robot i quantizes its analog measurement, $z_k^i \in \mathbb{R}$, to $b_k^i \in \mathcal{B}$, $\mathcal{B} := \{1, \dots, 2^f\}$ using the following quantization rule before broadcasting it:

$$b_k^i = \mathbf{q}[z_k^i], \quad \text{where } \mathbf{q}: \mathbb{R} \rightarrow \mathcal{B}. \quad (3)$$

Next, each robot uses a quantized filter, such as the BQKF or the IQKF [16], to generate MMSE estimates (under Gaussian assumption⁴) for the robots' poses using all quantized measurements, $\mathbf{b}_{0:k}$, up to time-step k . However, the quantization rules used by these filters depend upon the robots' pose estimates, via the measurement innovation, and thus all robots have to maintain *identical* filters to ensure estimation consistency. Therefore, even though each robot i has access to its own analog measurements, $\mathbf{z}_{0:k}^i$, it is forced to discard this information and process only the corresponding quantized measurements, $\mathbf{b}_{0:k}^i$.

III. HYBRID ESTIMATION FRAMEWORK

In order to address this problem, we introduced a novel hybrid estimation framework in [18] that enables each robot to process all available measurement information, i.e., *local analog* and *remote quantized* measurements. To achieve this, each robot i maintains two estimators (see

⁴It is important to note that this loss of Gaussianity in the IQKF and BQKF is due to the non-linearity of the quantization step as opposed to the non-linearity of the process and measurement models in the EKF.

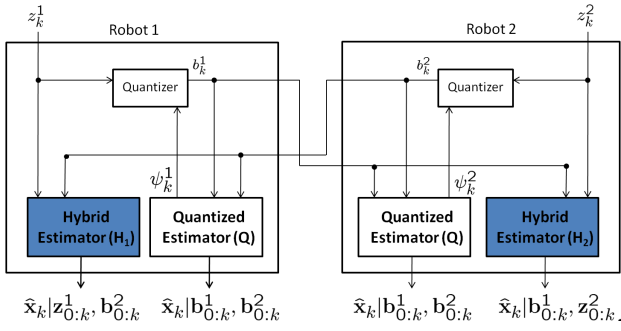


Fig. 1. Hybrid Estimation framework. When $\psi_k^i := E[z_k^i | \mathbf{b}_{0:k-1}]$ and we use the quantization rule in (4), the H- and Q-estimators correspond to the H-BQKF and BQKF, respectively. When $\psi_k^i := E[z_k^i | \mathbf{b}_{0:k-1}, \mathbf{b}_k^{i(1:p-1)}]$ and we use the quantization rule in (8), the H- and Q-estimators correspond to the H-IQKF and IQKF, respectively, $i = 1, 2$.

Fig. 1): (1) a quantized Q-estimator that processes quantized measurements from all robots including itself, i.e., $\hat{\mathbf{x}}_{k|k}^Q := E[\mathbf{x}_k | \mathbf{b}_{0:k}^{q \neq i}, \mathbf{b}_{0:k}^i]$, and (2) a hybrid H-estimator that processes its own analog measurements and quantized measurements from the other robots in the team, i.e., $\hat{\mathbf{x}}_{k|k}^{H_i} := E[\mathbf{x}_k | \mathbf{b}_{0:k}^{q \neq i}, \mathbf{z}_{0:k}^i]$, $q = 1, \dots, N$. The estimates generated by the Q-estimator are *identical* for all robots since each robot processes the same measurements, $\mathbf{b}_{0:k} = \{\mathbf{b}_{0:k}^{q \neq i}, \mathbf{b}_{0:k}^i\}$. Therefore, they are used in the hybrid estimation framework for generating quantization thresholds for all robots as shown in the next section. On the contrary, the estimates generated by the H-estimator are *different* for each robot, since each robot processes a different set of quantized and analog measurements.

In the next section, we derive MMSE (under Gaussian assumption) H-estimators that process: (i) local analog measurements, and (ii) multiple bits ($f \geq 1$), per analog measurement, communicated by other robots in the team. Specifically, we derive: (1) the H-BQKF for batch quantization, where the bandwidth availability (f bits per analog measurement) is known *a priori*, and (2) H-IQKF for iterative quantization, when additional bandwidth becomes available on-the-fly.

A. Batch Quantization

1) *Encoding rule (Quantizer design)*: Since robot j is pre-informed about the availability of $f \geq 1$ bits for communicating its analog measurement $z_k^j \in \mathbb{R}$, robot j partitions the observation space \mathbb{R} into 2^f intervals. The interval $\mathcal{R}_k^j(n) := [\tau_k^j(n), \tau_k^j(n+1))$, where $\tau_k^j(n)$ are the quantization thresholds, $n \in \mathcal{B} := \{1, \dots, 2^f\}$, $\tau_k^j(1) = -\infty$, $\tau_k^j(2^f + 1) = \infty$, and $\tau_k^j(n) < \tau_k^j(n+1)$. The quantization rule, which is based on the measurement innovation, has the form⁵ [16]:

$$b_k^j = n, \text{ iff } (z_k^j - E[z_k^j | \mathbf{b}_{0:k-1}, \mathbf{b}_k^m]) \in [\tau_k^j(n), \tau_k^j(n+1)) \quad (4)$$

⁵We assume a round-robin scheduling algorithm where the quantized measurements are generated and processed sequentially, based on robot ids. Therefore, robot i generates and communicates its quantized measurement, b_k^i , before robot $(i+1)$. Moreover, all robots in the team process b_k^i to obtain $\hat{\mathbf{x}}_{k|k}^Q$, before robot $(i+1)$ generates its quantized measurement.

where, $\mathbf{b}_{0:k-1}$ denotes the quantized measurements from all robots up to time-step $k-1$, and \mathbf{b}_k^m denotes the quantized measurements from robot m , $m = 1, \dots, (j-1)$, at time-step k . From (2), the predicted measurement is $E[z_k^j | \mathbf{b}_{0:k-1}, \mathbf{b}_k^m] =: \mathbf{h}_k^j \hat{\mathbf{x}}_{k|k,j-1}^Q$. Note that robot j uses the Q-estimator's predicted measurement, that is identical for all robots, for generating the quantized measurements. This allows other robots to correctly process/decode the quantized measurement. Robot j does *not* use the predicted measurement of its H-estimator, $E[z_k^j | \mathbf{b}_{0:k-1}^{q \neq j}, \mathbf{b}_k^m, \mathbf{z}_{0:k}^j]$, $q = 1, \dots, N$, since it depends upon its local analog measurements, $\mathbf{z}_{0:k}^j$, which are unavailable to the other robots.

2) *Decoding rule (Estimator design)*: For the batch quantization rule from (4), we now derive the resulting MMSE-based Q- and H-estimators. Note that the Q-estimator, by definition, is identical to the BQKF in [16] and is not presented here due to space constraints. The H-estimator, H-BQKF, is obtained as follows.

Proposition 1: H-estimator (H-BQKF)

Consider the linear model of (1)-(2) and the quantization rule in (4). If robot i assumes the posterior pdf $p[\mathbf{x}_{k-1} | \mathbf{b}_{0:k-1}^{q \neq i}, \mathbf{z}_{0:k-1}^i] \sim \mathcal{N}(\hat{\mathbf{x}}_{k-1|k-1}^{H_i}, \mathbf{P}_{k-1|k-1}^{H_i})$, then the state/covariance propagation equations from time-step $k-1$ to k are identical to the KF. If robot i , assumes the prior pdf $p[\mathbf{x}_k | \mathbf{b}_{0:k-1}^{q \neq i}, \mathbf{b}_k^{m \neq i}, \mathbf{z}_{0:k-1}^i] \sim \mathcal{N}(\hat{\mathbf{x}}_{k|k,j-1}^{H_i}, \mathbf{P}_{k|k,j-1}^{H_i})$, then the MMSE estimator for robot i processing its *own* analog measurement, z_k^i , is identical to the KF.

For the MMSE estimator processing the quantized measurement b_k^j from robot j , $j \neq i$, the state/covariance update equations are given by

$$\hat{\mathbf{x}}_{k|k,j}^{H_i} = \hat{\mathbf{x}}_{k|k,j-1}^{H_i} + \alpha_{H_i}(n) \frac{\mathbf{P}_{k|k,j-1}^{H_i} \mathbf{h}_k^j}{\sqrt{\mathbf{h}_k^{jT} \mathbf{P}_{k|k,j-1}^{H_i} \mathbf{h}_k^j + \sigma_k^2}} \quad (5)$$

$$\mathbf{P}_{k|k,j}^{H_i} = \mathbf{P}_{k|k,j-1}^{H_i} - \beta_{H_i}(n) \frac{\mathbf{P}_{k|k,j-1}^{H_i} \mathbf{h}_k^j \mathbf{h}_k^{jT} \mathbf{P}_{k|k,j-1}^{H_i}}{\mathbf{h}_k^{jT} \mathbf{P}_{k|k,j-1}^{H_i} \mathbf{h}_k^j + \sigma_k^2} \quad (6)$$

where

$$\alpha_{H_i}(n) = \frac{1}{\sqrt{2\pi}} \frac{\exp[-\Delta_{H_i}^2(n)/2] - \exp[-\Delta_{H_i}^2(n+1)/2]}{\mathcal{Q}[\Delta_{H_i}(n)] - \mathcal{Q}[\Delta_{H_i}(n+1)]}$$

$$\beta_{H_i}(n) = \alpha_{H_i}^2(n) - \frac{1}{\sqrt{2\pi}} \times \frac{\Delta_{H_i}(n) \exp[-\Delta_{H_i}^2(n)/2] - \Delta_{H_i}(n+1) \exp[-\Delta_{H_i}^2(n+1)/2]}{\mathcal{Q}[\Delta_{H_i}(n)] - \mathcal{Q}[\Delta_{H_i}(n+1)]}$$

$$\Delta_{H_i}(n) = \frac{(\tau_k^j(n) - \mathbf{h}_k^{jT} (\hat{\mathbf{x}}_{k|k,j-1}^{H_i} - \hat{\mathbf{x}}_{k|k,j-1}^Q))}{\sigma_{H_i}}$$

$$\sigma_{H_i}^2 = \mathbf{h}_k^{jT} \mathbf{P}_{k|k,j-1}^{H_i} \mathbf{h}_k^j + \sigma_k^2 \text{ and } 0 < \beta_{H_i}(n) < 1.$$

Proof: See Appendix. ■

3) *Quantization thresholds*: We now discuss the selection of optimal quantization thresholds, $\tau_k^j(n)$, $n = 2, \dots, 2^f$, for the batch quantized hybrid estimation framework. For the team to optimally and correctly process quantized measurements received from robot j , robot j 's quantization thresholds should be known to the team. Therefore, we choose robot j 's thresholds so as to maximize the average

reduction in the covariance of the Q-estimator, BQKF. Since the Q-estimator is identical for all robots, every robot in the team can locally calculate the quantization thresholds used by robot j . Thus, the threshold selection is an optimization problem of the form (see [16] for details):

$$\{\Delta_Q^*(n)\}_{n=2}^{2^f} := \arg \max_{\{\Delta_Q(n)\}_{n=2}^{2^f}} E[\beta_Q(n)|\mathbf{b}_{0:k-1}, \mathbf{b}_k^m] \quad (7)$$

where $\beta_Q(n)$ is a term, similar to $\beta_{H_i}(n)$ in (6), that appears in the covariance update equation of the BQKF (see [20] for detailed expression), and the expectation is with respect to the $Pr\{\mathbf{b}_{0:k-1}^j, \mathbf{b}_k^m\}$. Maximizing the average covariance reduction of the BQKF is equivalent to maximizing the expected value of $\beta_Q(n)$. Moreover, the optimization problem in (7) is equivalent to quantizing the measurement innovation, $z_k^j - \mathbf{h}_k^{jT} \hat{\mathbf{x}}_{k|k,j-1}^Q$, with minimum MSE distortion [16]. The solution to (7) is the well-known Lloyd-Max quantizer and the corresponding values for the optimal quantization thresholds can be found in [21], [22].

Before proceeding, we make the following important observations about the proposed H-BQKF:

- 1) As seen from Proposition 1, even though robot i cannot communicate its analog measurement, z_k^i , to the team, the H-BQKF enables it to *optimally* process this measurement locally using the KF.
- 2) Define $\bar{\alpha}_{H_i}(n) = \alpha_{H_i}(n) \sqrt{\mathbf{h}_k^{jT} \mathbf{P}_{k|k,j-1}^{H_i} \mathbf{h}_k^j + \sigma_k^2}$. Using this in (5), we see that the structure of the state update equation, for processing quantized measurements in H-BQKF, is very similar to that of the KF [15]. Moreover, as expected, the measurement innovation in the state update equation of the KF is approximated by $\bar{\alpha}_{H_i}(n)$ in the H-BQKF.
- 3) The structure of the covariance update equation [see (6)] for processing quantized measurements in the H-BQKF is identical to that of KF, except for the factor $\beta_{H_i}(n)$. Since $0 < \beta_{H_i}(n) < 1$, the covariance reduction for these estimators will always be less than that of the KF as measurement information is discarded during quantization.
- 4) While processing quantized measurements, the state/covariance update equations for the H-BQKF [see (5) and (6)] are a function of the difference between the predicted measurements, $\mathbf{h}_k^{jT} \hat{\mathbf{x}}_{k|k,j-1}^{H_i}$ and $\mathbf{h}_k^{jT} \hat{\mathbf{x}}_{k|k,j-1}^Q$, of the H-BQKF and BQKF respectively. Moreover, the covariance reduction in (6) increases as the absolute value of this difference decreases. This is because the quantized measurements are generated using the BQKF's predicted measurement [see (4)]. If the difference between the predicted measurements of the H-BQKF and BQKF is large, the quantized measurement will convey very little information to the H-BQKF.
- 5) By choosing $f = 1$ and substituting the corresponding optimal thresholds $\tau_k^j(1) = -\infty$, $\tau_k^j(2) = 0$, and $\tau_k^j(3) = \infty$ in Proposition 1, we obtain the special case of the single bit H-estimator in [18].

B. Iterative Quantization

1) *Encoding rule (Quantizer design)*: When additional communication bandwidth becomes available to the robots on-the-fly, robot j can now communicate extra bits, *one bit at a time*, for the same analog measurement z_k^j . If robot j has communicated $(p-1)$ bits, $\mathbf{b}_k^{j(1:p-1)}$, $p \geq 1$, for the analog measurement z_k^j , then robot j generates the p -th bit, $b_k^{j(p)}$, using the following quantization rule

$$b_k^{j(p)} := \text{sign}[z_k^j - E[z_k^j | \mathbf{b}_{0:k-1}, \mathbf{b}_k^m, \mathbf{b}_k^{j(1:p-1)}]] \quad (8)$$

where, $\mathbf{b}_{0:k-1}$ denotes the quantized bits from all robots up to time-step $k-1$, and \mathbf{b}_k^m denotes the quantized measurements from robot m , $m = 1, \dots, (j-1)$, at time-step k . The expected measurement is given by

$$\begin{aligned} & E[z_k^j | \mathbf{b}_{0:k-1}, \mathbf{b}_k^m, \mathbf{b}_k^{j(1:p-1)}] \\ &= E[\mathbf{h}_k^{jT} \mathbf{x}_k + v_k^j | \mathbf{b}_{0:k-1}, \mathbf{b}_k^m, \mathbf{b}_k^{j(1:p-1)}] \\ &= \mathbf{h}_k^{jT} E[\mathbf{x}_k | \mathbf{b}_{0:k-1}, \mathbf{b}_k^m, \mathbf{b}_k^{j(1:p-1)}] \\ &\quad + E[v_k^j | \mathbf{b}_{0:k-1}, \mathbf{b}_k^m, \mathbf{b}_k^{j(1:p-1)}] \\ &= \mathbf{h}_k^{jT} \hat{\mathbf{x}}_{k|k,j}^{Q(p-1)} + E[v_k^j | \mathbf{b}_{0:k-1}, \mathbf{b}_k^m, \mathbf{b}_k^{j(1:p-1)}]. \end{aligned} \quad (9)$$

Importantly, in the above equation, the term $E[v_k^j | \mathbf{b}_{0:k-1}, \mathbf{b}_k^m, \mathbf{b}_k^{j(1:p-1)}] \neq 0$, unless $p = 1$. If $p > 1$, the measurement noise, v_k^j , is no longer independent of the previous bits, $\mathbf{b}_k^{j(1:p-1)}$, since they were generated using the noisy analog measurement, z_k^j , itself. Therefore, the MMSE estimates of the noise term are needed to correctly generate/decode the bits. These estimates can be obtained by augmenting the state, \mathbf{x}_k , with the noise term, v_k^j , and considering the augmented state vector $\check{\mathbf{x}}_k = [\mathbf{x}_k^T, v_k^j]^T$ and a modified $\check{\mathbf{h}}_k^j = [\mathbf{h}_k^j, 1]^T$. With these changes, the process and measurement models from (1)-(2) can be rewritten as [16]:

$$\begin{aligned} \check{\mathbf{x}}_k &= \check{\mathbf{F}}_{k-1} \check{\mathbf{x}}_{k-1} + \check{\mathbf{G}}_{k-1} \check{\mathbf{w}}_{k-1}, \quad z_k^j = \check{\mathbf{h}}_k^{jT} \check{\mathbf{x}}_k \\ \text{where } \check{\mathbf{F}}_{k-1} &:= \begin{bmatrix} \mathbf{F}_{k-1} & \mathbf{0} \\ \mathbf{0}^T & 0 \end{bmatrix}, \quad \check{\mathbf{G}}_{k-1} := \begin{bmatrix} \mathbf{G}_{k-1} & \mathbf{0} \\ \mathbf{0}^T & 1 \end{bmatrix}, \\ \check{\mathbf{w}}_{k-1} &:= [\mathbf{w}_{k-1}^T, v_{k-1}^j]^T, \\ \check{\mathbf{Q}}_{k-1} &:= E[\check{\mathbf{w}}_{k-1} \check{\mathbf{w}}_{k-1}^T] = \begin{bmatrix} \mathbf{Q}_{k-1} & \mathbf{0} \\ \mathbf{0}^T & \sigma_k^2 \end{bmatrix} \end{aligned} \quad (10)$$

Thus, every time robot i generates its own iteratively quantized measurements or processes iteratively quantized bits communicated by other robots, it has to augment its own state vector with the corresponding measurement noise so that the noise statistics can be correctly estimated. Then the quantization process in (8) becomes identical to that of the sign-of-innovation quantization rule from [14].

2) *Decoding rule (Estimator design)*: For the iterative quantization rule in (8), we now derive the Q- and H-estimators. The Q-estimator, *by definition*, is identical to the IQKF presented in [16] and is not presented here due to space constraints. The H-estimator, H-IQKF, is obtained as follows.

Proposition 2: H-estimator (H-IQKF)

Consider the linear model of (10) and the quantization rule in (8). If robot i assumes the posterior pdf $p[\hat{\mathbf{x}}_{k-1} | \mathbf{b}_{0:k-1}^{q \neq i}, \mathbf{z}_{0:k-1}^i] \sim \mathcal{N}(\hat{\mathbf{x}}_{k-1|k-1}^{H_i}, \check{\mathbf{P}}_{k-1|k-1}^{H_i})$, the state/covariance propagation equations are given by

$$\hat{\mathbf{x}}_{k|k-1}^{H_i} = \check{\mathbf{F}}_{k-1} \hat{\mathbf{x}}_{k-1|k-1}^{H_i} \quad (11)$$

$$\check{\mathbf{P}}_{k|k-1}^{H_i} = \check{\mathbf{F}}_{k-1} \check{\mathbf{P}}_{k-1|k-1}^{H_i} \check{\mathbf{F}}_{k-1}^T + \check{\mathbf{G}}_{k-1} \check{\mathbf{Q}}_{k-1} \check{\mathbf{G}}_{k-1}^T. \quad (12)$$

If robot i assumes the pdf $p[\hat{\mathbf{x}}_k | \mathbf{b}_{0:k-1}^{q \neq i}, \mathbf{z}_{0:k-1}^i, \mathbf{b}_k^{m \neq i}, \mathbf{b}_k^{j(1:p-1)}] \sim \mathcal{N}(\hat{\mathbf{x}}_{k|k,j}^{H_i(p-1)}, \check{\mathbf{P}}_{k|k,j}^{H_i(p-1)})$, then the MMSE estimator for robot i processing its own analog measurement, z_k^i , is identical to the KF.

For the MMSE estimator for robot i , that processes the quantized measurement, $b_k^{j(p)}$, $j \neq i$, from robot j , the state/covariance update equations are given by

$$\hat{\mathbf{x}}_{k|k,j}^{H_i(p)} = \hat{\mathbf{x}}_{k|k,j}^{H_i(p-1)} + \alpha \frac{\check{\mathbf{P}}_{k|k,j}^{H_i(p-1)} \check{\mathbf{h}}_k^j b_k^{j(p)}}{\sqrt{\check{\mathbf{h}}_k^{jT} \check{\mathbf{P}}_{k|k,j}^{H_i(p-1)} \check{\mathbf{h}}_k^j}} b_k^{j(p)} \quad (13)$$

$$\check{\mathbf{P}}_{k|k,j}^{H_i(p)} = \check{\mathbf{P}}_{k|k,j}^{H_i(p-1)} - \beta \frac{\check{\mathbf{P}}_{k|k,j}^{H_i(p-1)} \check{\mathbf{h}}_k^j \check{\mathbf{h}}_k^{jT} \check{\mathbf{P}}_{k|k,j}^{H_i(p-1)}}{\check{\mathbf{h}}_k^{jT} \check{\mathbf{P}}_{k|k,j}^{H_i(p-1)} \check{\mathbf{h}}_k^j} \quad (14)$$

where,

$$\alpha = \frac{\exp[-\Delta^2/2]}{\sqrt{2\pi}Q[-b_k^{j(p)}\Delta]}, \quad \beta = \alpha^2 + b_k^{j(p)} \frac{\Delta \exp[-\Delta^2/2]}{\sqrt{2\pi}Q[-b_k^{j(p)}\Delta]}$$

$$\Delta = \frac{\check{\mathbf{h}}_k^{jT} (\hat{\mathbf{x}}_{k|k,j}^{H_i(p-1)} - \hat{\mathbf{x}}_{k|k,j}^{Q(p-1)})}{\sqrt{\check{\mathbf{h}}_k^{jT} \check{\mathbf{P}}_{k|k,j}^{H_i(p-1)} \check{\mathbf{h}}_k^j}}$$

Proof: This proof is similar to that of Proposition 1 and is presented in [20]. ■

Note that the first $r = 3N$ elements of $\hat{\mathbf{x}}_{k|k,j}^{Q(p)}$ and $\hat{\mathbf{x}}_{k|k,j}^{H_i(p)}$ correspond to the robots' state estimates, and the top $r \times r$ sub-matrices of $\check{\mathbf{P}}_{k|k,j}^{Q(p)}$ and $\check{\mathbf{P}}_{k|k,j}^{H_i(p)}$ correspond to their covariance, respectively. Once all bits corresponding to z_k^j have been processed, the robots can revert to the original state vector, \mathbf{x}_k . When processing bits from a new analog measurement, the robots will again augment the state with the corresponding measurement noise and the above procedure will be repeated.

From Proposition 2, we see that even though robot i cannot communicate its analog measurement, z_k^i , to the team, the H-IQKF enables it to *optimally* process this measurement locally using the KF. Next, note that the structures of the IQKF and H-IQKF, are strikingly similar to that of the single-bit SOI-KF [14] and H-SOIKF [18], respectively, where the analog measurement is quantized to a single bit. Specifically, as expected, when $p = 1$, the IQKF and H-IQKF are identical to SOI-KF and H-SOIKF, respectively. Moreover, the structure of the IQKF and H-IQKF is similar to that of the KF, and as expected, the covariance reduction of these quantized-innovation filters is smaller than that of the KF. Lastly, similar to the H-BQKF, when the H-IQKF processes quantized measurements, the state/covariance update equations are a function of the difference between the

predicted measurements, $\check{\mathbf{h}}_k^{jT} \hat{\mathbf{x}}_{k|k,j}^{H_i(p-1)}$ and $\check{\mathbf{h}}_k^{jT} \hat{\mathbf{x}}_{k|k,j}^{Q(p-1)}$, of the H-IQKF and IQKF, respectively.

IV. SIMULATIONS AND EXPERIMENT

A. Simulation Results

The simulation set-up consists of a team of two robots navigating in 2D while performing MC-CL. The continuous-time dynamics for each robot are given by the constant velocity motion model [19]:

$$\dot{\mathbf{x}} = \mathbf{f}(\mathbf{x}) + \mathbf{G}_c \begin{bmatrix} w_v \\ w_\omega \end{bmatrix} \quad (15)$$

where $\mathbf{x} = [x, y, \phi, v, \omega]^T$, $\mathbf{f}(\mathbf{x}) = [v \cos \phi, v \sin \phi, \omega, 0, 0]^T$ and $\mathbf{G}_c = [\mathbf{0}_{2 \times 3}, \mathbf{I}_{2 \times 2}]^T$. The standard deviation of the continuous-time noise in the linear, v , and rotational, ω , velocity is chosen to be $\sigma_v = 0.6325$ m/s. $\sqrt{\text{Hz}}$ and $\sigma_\omega = 0.4967$ rad/s. $\sqrt{\text{Hz}}$ respectively. Each robot obtains measurements for its linear, v_m , and rotational, ω_m , velocity, as well as its distance, d_m , and bearing, θ_m , to the other robot. The noise in these measurements is modeled as zero-mean, white Gaussian with standard deviation $\sigma_{v_m} = 0.07$ m/s, $\sigma_{\omega_m} = 0.28$ rad/s for the linear and rotational velocity measurements, respectively, and $\sigma_{d_m} = 0.05$ m, $\sigma_{\theta_m} = 0.09$ rad for the corresponding distance and bearing measurements.

In this section, we compare the performance of the proposed H-estimators (process local analog and remote quantized measurements), H-BQKF and H-IQKF, with: (1) the Q-estimators (process local and remote quantized measurements), BQKF and IQKF, using 1–4 bits per remote analog measurement, and (2) the standard EKF that uses analog measurements from all robots and hence is our benchmark. Figures 2, 3 show the root mean squared error (RMSE) in

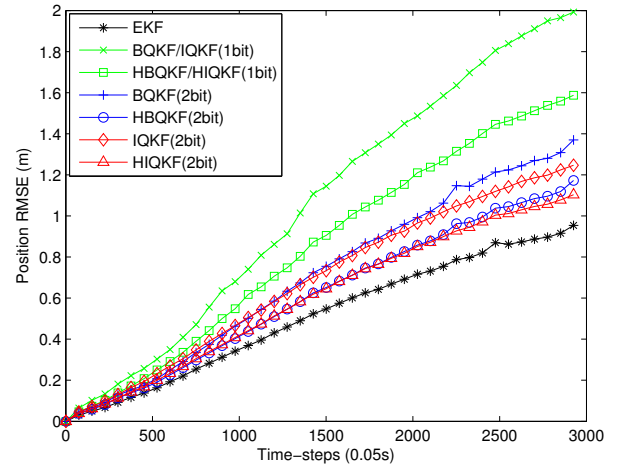


Fig. 2. Comparison of position RMSE for EKF, and 1–2 bit H-BQKF, H-IQKF, BQKF, and IQKF.

the position and orientation estimates for these estimators, averaged over the 2 robots and 100 Monte Carlo trials. For clarity, we have included only the results for $n = 1, 2$ bits. Since the estimates generated by the H-estimator are different

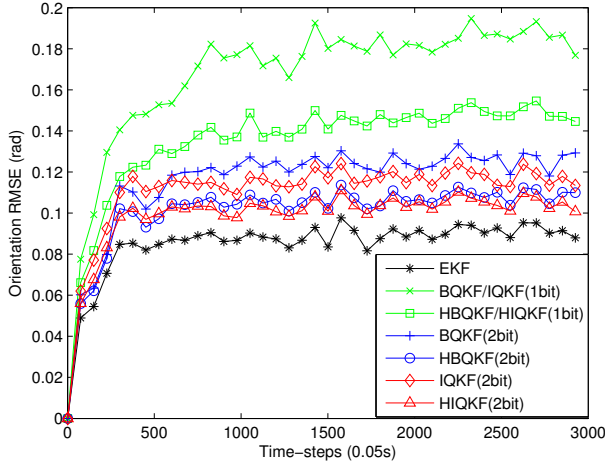


Fig. 3. Comparison of orientation RMSE for EKF, and 1 – 2 bit H-BQKF, H-IQKF, BQKF, and IQKF.

for each robot, the RMSE for the H-estimators, H-BQKF and H-IQKF, are also averaged over estimators maintained by each robot. Table I, presents the results for position and orientation RMSE, for $n = 1, 2, 4$ bits, averaged over the duration of the simulation run. Moreover, since the 1-bit iterative- and batch-quantized estimators are identical, Table I omits the results for the 1-bit iteratively quantized filters.

From Figs. 2, 3, and Table I, we observe that the estimates generated by the proposed H-estimators, H-BQKF and H-IQKF, are more accurate than their Q-estimator counterparts, BQKF and IQKF, irrespective of the number of quantization bits ($n = \{1, 2, 4\}$) considered. Specifically, the 1-bit hybrid filters are 20% more accurate than the 1-bit quantized filters, while the 2-bit hybrid filters show a performance improvement of 13% over their quantized counterparts. Overall, the error in the estimates decreases as we increase the number of quantization bits and by communicating as few as 4 bits per analog measurement, both the H- and Q-estimators are able to achieve accuracy very close to that of the analog EKF. Also, for a fixed number of bits, the performance of both the batch and iteratively quantized estimators is comparable. Thus, we conclude that by including their local analog measurements in the estimation process, without any additional communication overhead, the robots are able to substantially improve the estimation accuracy of CL.

B. Experimental Results

Experimental validation was carried out using a team of four Pioneer-I robots moving in a rectangular arena of $4 \text{ m} \times 2.5 \text{ m}$ for approximately 16 minutes. An overhead camera is used to obtain the robots' poses in a global coordinate frame (ground truth).

The robots move with a constant velocity of 0.1 m/s while avoiding collisions with the boundaries of the arena and other robots in the team. The robots obtain linear and rotational velocity (odometry) measurements, and relative distance and bearing measurements at a frequency of 1 Hz. The noise standard deviations of the odometry

TABLE I
SIMULATION RESULTS FOR $N = 2$ ROBOTS

	Pos. RMSE (m)	Orient. RMSE (rad)
BQKF (1 bit):	1.0743	0.1689
H-BQKF (1 bit):	0.8584	0.1361
BQKF (2 bit):	0.7203	0.1171
H-BQKF (2 bit):	0.6199	0.1018
BQKF (4 bit):	0.5515	0.0910
H-BQKF (4 bit):	0.5337	0.0885
IQKF (2 bit):	0.6932	0.1120
H-IQKF (2 bit):	0.6105	0.0997
IQKF (4 bit):	0.6176	0.1007
H-IQKF (4 bit):	0.5673	0.0934
EKF (analog):	0.5151	0.0858

measurements for the heterogeneous robot team vary from 0.0078 rad/s to 0.02 rad/s for rotational velocity, and from 0.0032 m/s to 0.0059 m/s for linear velocity. The relative distance and bearing measurements between the robots are generated synthetically using data from the overhead camera and adding Gaussian noise with standard deviation $\sigma_d = 0.05 \text{ m}$ for distance and $\sigma_\theta = 2 \text{ deg}$ for relative bearing. Table II, presents the position and orientation RMSE for each

TABLE II
EXPERIMENTAL RESULTS FOR THE HYBRID ESTIMATION FRAMEWORK

	RMS Position error (m)			
	Robot 1	Robot 2	Robot 3	Robot 4
BQKF (1 bit):	1.3643	1.1973	1.2849	1.1794
H-BQKF (1 bit):	1.0254	0.9358	0.9716	0.9714
BQKF (2 bit):	0.8654	0.7405	0.8383	0.8752
H-BQKF (2 bit):	0.7516	0.6652	0.7254	0.7542
BQKF (3 bit):	0.5330	0.4824	0.5168	0.4742
H-BQKF (3 bit):	0.5821	0.5553	0.5665	0.5809
IQKF (2 bit):	0.5990	0.5961	0.5758	0.7062
H-IQKF (2 bit):	0.6023	0.5879	0.5870	0.6637
IQKF (3 bit):	0.6255	0.6187	0.6291	0.7028
H-IQKF (3 bit):	0.5770	0.5547	0.5650	0.5974
EKF (analog):	0.5651	0.5385	0.5239	0.5719
	RMS Orientation error (rad)			
	Robot 1	Robot 2	Robot 3	Robot 4
BQKF (1 bit):	0.7793	0.7810	0.7777	0.7820
H-BQKF (1 bit):	0.6331	0.6337	0.6289	0.6345
BQKF (2 bit):	0.6305	0.6314	0.6294	0.6296
H-BQKF (2 bit):	0.5392	0.5402	0.5386	0.5385
BQKF (3 bit):	0.3182	0.3174	0.3171	0.3176
H-BQKF (3 bit):	0.4064	0.4062	0.4059	0.4058
IQKF (2 bit):	0.4530	0.4549	0.4540	0.4543
H-IQKF (2 bit):	0.4300	0.4316	0.4306	0.4314
IQKF (3 bit):	0.4480	0.4468	0.4461	0.4465
H-IQKF (3 bit):	0.3812	0.3802	0.3795	0.3796
EKF (analog):	0.4055	0.4064	0.4059	0.4060

robot, averaged over all time-steps. For the H-estimators, these quantities are also averaged across all robot's H-estimators. From the RMSE data in the table, we conclude that the n -bit, $n = \{1, 2\}$, H-estimators (H-BQKF and H-IQKF) outperform the corresponding Q-estimators (BQKF and IQKF). Thus the H-estimators, by enabling robots to

include their local analog measurements in the estimation process, significantly improve the estimation accuracy of CL. Specifically, the improvement in performance of the H-estimators over the Q-estimators is more pronounced for the $n = 1, 2$ bit scenario, while with $n = 3$ bits, the performance of both the Q- and H-estimators is very close to that of the standard analog EKF. For this particular experiment, we observe that the RMSE of the 3-bit BQKF is lower than that of both the 3-bit H-BQKF and the EKF. Moreover, the RMSE for the 3-bit H-IQKF is lower than that of the EKF. However, these results are reported for a single experimental run, and in general, we would expect the H-estimators to outperform the corresponding Q-estimators and the EKF to outperform all the Q- and H-estimators. To study the consistency of these estimators, the results from the normalized estimation error squared (NEES) test are available in [20].

V. CONCLUSIONS AND FUTURE WORK

In this paper, we derived two MMSE-based estimators for the hybrid estimation framework, the H-BQKF and the H-IQKF, that can process local analog measurements along with $f \geq 1$ bits per remote analog measurement, in order to improve the estimation accuracy of CL under time-varying communication-bandwidth constraints. We tested the performance and accuracy of the proposed multi-bit hybrid filters for the CL application in simulations and experiment and showed that they outperform the existing multi-bit quantized filters, BQKF and IQKF. As part of our future work, we plan to analytically evaluate the performance of the proposed H-BQKF and the H-IQKF. Furthermore, we will also rigorously analyze the effect of packet-loss and communication errors on the performance of the proposed estimators.

APPENDIX

We now present an outline of the proof for the H-BQKF. Due to space constraints, additional mathematical details of the derivation can be found in [20].

Under the Gaussian assumption for the pdf $p[\mathbf{x}_{k-1} | \mathbf{b}_{0:k-1}^{q \neq i}, \mathbf{z}_{0:k-1}^i]$, the state and covariance propagation derivations are identical to the standard KF [15]. When robot i processes its own analog measurement z_k^i , the state/covariance update derivations proceed as follows:

$$\begin{aligned} E[\mathbf{x}_k | \mathbf{b}_{0:k-1}^{q \neq i}, \mathbf{b}_k^{m \neq i}, \mathbf{z}_{0:k}^i] &= \int_{\mathbb{R}^{3N}} \mathbf{x}_k p(\mathbf{x}_k | \mathbf{b}_{0:k-1}^{q \neq i}, \mathbf{b}_k^{m \neq i}, \mathbf{z}_{0:k}^i) d\mathbf{x}_k \\ &= \int_{\mathbb{R}^{3N}} \mathbf{x}_k \left(\frac{p(z_k^i | \mathbf{x}_k, \mathbf{b}_{0:k-1}^{q \neq i}, \mathbf{b}_k^{m \neq i}, \mathbf{z}_{0:k-1}^i)}{p(z_k^i | \mathbf{b}_{0:k-1}^{q \neq i}, \mathbf{b}_k^{m \neq i}, \mathbf{z}_{0:k-1}^i)} \right. \\ &\quad \left. \times p(\mathbf{x}_k | \mathbf{b}_{0:k-1}^{q \neq i}, \mathbf{b}_k^{m \neq i}, \mathbf{z}_{0:k-1}^i) \right) d\mathbf{x}_k \quad (16) \end{aligned}$$

In the above equation, $p(z_k^i | \mathbf{x}_k, \mathbf{b}_{0:k-1}^{q \neq i}, \mathbf{b}_k^{m \neq i}, \mathbf{z}_{0:k-1}^i) \sim \mathcal{N}(\mathbf{h}_k^{i^T} \mathbf{x}_k, \sigma_k^{i^2})$ and $p(z_k^i | \mathbf{b}_{0:k-1}^{q \neq i}, \mathbf{b}_k^{m \neq i}, \mathbf{z}_{0:k-1}^i) \sim \mathcal{N}(\mathbf{h}_k^{i^T} \hat{\mathbf{x}}_{k|k,j-1}^{H_i}, \mathbf{h}_k^{i^T} \mathbf{P}_{k|k,j-1}^{H_i} \mathbf{h}_k^i + \sigma_k^{i^2})$. Therefore, all pdfs in (16) are Gaussian, similar to that of the KF. The derivation from this point onwards, is identical to that of the KF and can be found in [15].

To obtain the state/covariance update equations when processing quantized measurements received from other robots, we use the following concept of iterated expectation [23]:

$$E[g(\mathbf{x}) | y \in \mathcal{R}_i] = E[E[g(\mathbf{x}) | Y] | y \in \mathcal{R}_i] \quad (17)$$

where $g(\mathbf{x})$ is a function of the random variable $\mathbf{x} \in \mathbb{R}^r$, Y is a random variable in \mathbb{R} , y is its realization, and $\mathcal{R}_i \subseteq \mathbb{R}$.

We define the random variable $\tilde{z}_k^j = z_k^j - E[z_k^j | \mathbf{b}_{0:k-1}, \mathbf{b}_k^m]$. From (4), we see that b_k^j is a realization of the random variable \tilde{z}_k^j , i.e., when $b_k^j = n$, $\mathcal{R}_k^j(n) := [\tau_k^j(n), \tau_k^j(n+1))$ and $\tilde{z}_k^j \in \mathcal{R}_k^j(n)$. Therefore, when robot i is processing the quantized measurement $b_k^j = n$ from robot j , $j \neq i$, the state update, using (17), can be written as:

$$\begin{aligned} E[\mathbf{x}_k | \mathbf{b}_{0:k-1}^{q \neq i}, \mathbf{b}_k^{m \neq i}, \mathbf{z}_{0:k-1}^i, b_k^j] \\ = E[E[\mathbf{x}_k | \mathbf{b}_{0:k-1}^{q \neq i}, \mathbf{b}_k^{m \neq i}, \mathbf{z}_{0:k-1}^i, \tilde{z}_k^j] | \mathbf{b}_{0:k-1}^{q \neq i}, \mathbf{b}_k^{m \neq i}, \mathbf{z}_{0:k-1}^i, b_k^j] \end{aligned} \quad (18)$$

We first evaluate the inner expectation in the above equation. For this, we compute the joint pdf $p(\mathbf{x}_k, \tilde{z}_k^j | \mathbf{b}_{0:k-1}^{q \neq i}, \mathbf{b}_k^{m \neq i}, \mathbf{z}_{0:k-1}^i)$ and then obtain the desired conditional pdf $p(\mathbf{x}_k | \mathbf{b}_{0:k-1}^{q \neq i}, \mathbf{b}_k^{m \neq i}, \mathbf{z}_{0:k-1}^i, \tilde{z}_k^j)$. This joint pdf (under the Gaussian assumptions stated in Proposition 1) is also Gaussian and given by:

$$\begin{aligned} p(\mathbf{x}_k, \tilde{z}_k^j | \mathbf{b}_{0:k-1}^{q \neq i}, \mathbf{b}_k^{m \neq i}, \mathbf{z}_{0:k-1}^i) \sim \mathcal{N} \left(\begin{bmatrix} \hat{\mathbf{x}}_{k|k,j-1}^{H_i} \\ \mathbf{h}_k^{j^T} (\hat{\mathbf{x}}_{k|k,j-1}^{H_i} - \hat{\mathbf{x}}_{k|k,j-1}^Q) \end{bmatrix} \right. \\ \left. , \begin{bmatrix} \mathbf{P}_{k|k,j-1}^{H_i} & \mathbf{P}_{k|k,j-1}^{H_i} \mathbf{h}_k^j \\ \mathbf{h}_k^{j^T} \mathbf{P}_{k|k,j-1}^{H_i} & \mathbf{h}_k^{j^T} \mathbf{P}_{k|k,j-1}^{H_i} \mathbf{h}_k^j + \sigma_k^{j^2} \end{bmatrix} \right) \quad (19) \end{aligned}$$

From (19), we can obtain the mean and covariance of the conditional pdf as:

$$\begin{aligned} E[\mathbf{x}_k | \mathbf{b}_{0:k-1}^{q \neq i}, \mathbf{b}_k^{m \neq i}, \mathbf{z}_{0:k-1}^i, \tilde{z}_k^j] \\ = \hat{\mathbf{x}}_{k|k,j-1}^{H_i} + \mathbf{k}^c (\tilde{z}_k^j - \mathbf{h}_k^{j^T} (\hat{\mathbf{x}}_{k|k,j-1}^{H_i} - \hat{\mathbf{x}}_{k|k,j-1}^Q)) := \hat{\mathbf{x}}_{k|k,j-1}^{H_i^c} \\ \text{Cov}[\mathbf{x}_k | \mathbf{b}_{0:k-1}^{q \neq i}, \mathbf{b}_k^{m \neq i}, \mathbf{z}_{0:k-1}^i, \tilde{z}_k^j] = \mathbf{P}_{k|k,j-1}^{H_i} - \mathbf{k}^c \mathbf{h}_k^{j^T} \mathbf{P}_{k|k,j-1}^{H_i} \\ \text{where } \mathbf{k}^c = \frac{\mathbf{P}_{k|k,j-1}^{H_i} \mathbf{h}_k^j}{\mathbf{h}_k^{j^T} \mathbf{P}_{k|k,j-1}^{H_i} \mathbf{h}_k^j + \sigma_k^{j^2}}. \quad (20) \end{aligned}$$

Substituting (20) in (18), we obtain:

$$\begin{aligned} E[\mathbf{x}_k | \mathbf{b}_{0:k-1}^{q \neq i}, \mathbf{b}_k^{m \neq i}, \mathbf{z}_{0:k-1}^i, b_k^j] &= \hat{\mathbf{x}}_{k|k,j-1}^{H_i} + \\ \mathbf{k}^c E[\tilde{z}_k^j | \mathbf{b}_{0:k-1}^{q \neq i}, \mathbf{b}_k^{m \neq i}, \mathbf{z}_{0:k-1}^i, b_k^j] &- \mathbf{k}^c \mathbf{h}_k^{j^T} (\hat{\mathbf{x}}_{k|k,j-1}^{H_i} - \hat{\mathbf{x}}_{k|k,j-1}^Q) \end{aligned} \quad (21)$$

In order to evaluate $E[\tilde{z}_k^j | \mathbf{b}_{0:k-1}^{q \neq i}, \mathbf{b}_k^{m \neq i}, \mathbf{z}_{0:k-1}^i, b_k^j]$ in (21), we first consider the corresponding pdf which can be expressed as:

$$\begin{aligned} p(\tilde{z}_k^j | \mathbf{b}_{0:k-1}^{q \neq i}, \mathbf{b}_k^{m \neq i}, \mathbf{z}_{0:k-1}^i, b_k^j = n) \\ = p(\tilde{z}_k^j | \mathbf{b}_{0:k-1}^{q \neq i}, \mathbf{b}_k^{m \neq i}, \mathbf{z}_{0:k-1}^i, \tilde{z}_k^j \in \mathcal{R}_k^j(n)) \\ = \frac{p(\tilde{z}_k^j | \mathbf{b}_{0:k-1}^{q \neq i}, \mathbf{b}_k^{m \neq i}, \mathbf{z}_{0:k-1}^i)}{\Pr\{\tilde{z}_k^j \in \mathcal{R}_k^j(n) | \mathbf{b}_{0:k-1}^{q \neq i}, \mathbf{b}_k^{m \neq i}, \mathbf{z}_{0:k-1}^i\}} \mathbb{1}_{\tilde{z}_k^j \in \mathcal{R}_k^j(n)}, \text{ else } 0. \end{aligned} \quad (22)$$

Therefore,

$$E[\tilde{z}_k^j | \mathbf{b}_{0:k-1}^{q \neq i}, \mathbf{b}_k^{m \neq i}, \mathbf{z}_{0:k-1}^i, b_k^j = n] \\ = \int_{\mathcal{R}_k^j(n)} \tilde{z}_k^j \frac{p(\tilde{z}_k^j | \mathbf{b}_{0:k-1}^{q \neq i}, \mathbf{b}_k^{m \neq i}, \mathbf{z}_{0:k-1}^i)}{\Pr\{\tilde{z}_k^j \in \mathcal{R}_k^j(n) | \mathbf{b}_{0:k-1}^{q \neq i}, \mathbf{b}_k^{m \neq i}, \mathbf{z}_{0:k-1}^i\}} d\tilde{z}_k^j \quad (23)$$

Furthermore, in the above equation,

$$p(\tilde{z}_k^j | \mathbf{b}_{0:k-1}^{q \neq i}, \mathbf{b}_k^{m \neq i}, \mathbf{z}_{0:k-1}^i) \\ \sim \mathcal{N}\left(\mathbf{h}_k^{jT} (\hat{\mathbf{x}}_{k|k,j-1}^{H_i} - \hat{\mathbf{x}}_{k|k,j-1}^Q), \mathbf{h}_k^{jT} \mathbf{P}_{k|k,j-1}^{H_i} \mathbf{h}_k^j + \sigma_k^{j2}\right) \quad (24)$$

and

$$\Pr\{\tilde{z}_k^j \in \mathcal{R}_k^j(n) | \mathbf{b}_{0:k-1}^{q \neq i}, \mathbf{b}_k^{m \neq i}, \mathbf{z}_{0:k-1}^i\} \\ = \Pr\{\tau_k^j(n) \leq \tilde{z}_k^j < \tau_k^j(n+1) | \mathbf{b}_{0:k-1}^{q \neq i}, \mathbf{b}_k^{m \neq i}, \mathbf{z}_{0:k-1}^i\} \\ = \mathbf{Q}\left[\frac{\tau_k^j(n) - m}{\sigma_{H_i}}\right] - \mathbf{Q}\left[\frac{\tau_k^j(n+1) - m}{\sigma_{H_i}}\right] \quad (25)$$

Here, we define $m := \mathbf{h}_k^{jT} (\hat{\mathbf{x}}_{k|k,j-1}^{H_i} - \hat{\mathbf{x}}_{k|k,j-1}^Q)$ and $\sigma_{H_i}^2 := \mathbf{h}_k^{jT} \mathbf{P}_{k|k,j-1}^{H_i} \mathbf{h}_k^j + \sigma_k^{j2}$. Also, $\mathbf{Q}[\cdot]$ is the Gaussian tail probability function with $\mathbf{Q}[x] \triangleq \frac{1}{\sqrt{2\pi}} \int_x^\infty \exp(-u^2/2) du$, and if $Y \sim \mathcal{N}(\mu, \sigma^2)$, then $\Pr\{Y > y\} = \mathbf{Q}[(y - \mu)/\sigma]$.

After evaluating (23) using (24) and (25), the details of which are available in [20], the expression in (21) can be simplified to obtain the state update equation in (5).

The derivation for the corresponding covariance update equation is also based on the concept of iterated expectations [see (17)] as follows:

$$\text{Cov}[\mathbf{x}_k | \mathbf{b}_{0:k-1}^{q \neq i}, \mathbf{b}_k^{m \neq i}, \mathbf{z}_{0:k-1}^i, b_k^j] \\ = E[(\mathbf{x}_k - \hat{\mathbf{x}}_{k|k,j}^{H_i})(\mathbf{x}_k - \hat{\mathbf{x}}_{k|k,j}^{H_i})^T | \mathbf{b}_{0:k-1}^{q \neq i}, \mathbf{b}_k^{m \neq i}, \mathbf{z}_{0:k-1}^i, b_k^j] \\ = E[E[(\mathbf{x}_k - \hat{\mathbf{x}}_{k|k,j}^{H_i})(\mathbf{x}_k - \hat{\mathbf{x}}_{k|k,j}^{H_i})^T \\ | \mathbf{b}_{0:k-1}^{q \neq i}, \mathbf{b}_k^{m \neq i}, \mathbf{z}_{0:k-1}^i, \tilde{z}_k^j] | \mathbf{b}_{0:k-1}^{q \neq i}, \mathbf{b}_k^{m \neq i}, \mathbf{z}_{0:k-1}^i, b_k^j] \quad (26)$$

To evaluate the above expectation, the term $\mathbf{x}_k - \hat{\mathbf{x}}_{k|k,j}^{H_i}$, using (20) and (21), can be written as:

$$\mathbf{x}_k - \hat{\mathbf{x}}_{k|k,j}^{H_i} = \mathbf{x}_k - \hat{\mathbf{x}}_{k|k,j}^{H_i} + \hat{\mathbf{x}}_{k|k,j}^{H_i^c} - \hat{\mathbf{x}}_{k|k,j}^{H_i^c} \\ = \mathbf{x}_k - \hat{\mathbf{x}}_{k|k,j}^{H_i^c} + \mathbf{k}^c \left(\tilde{z}_k^j - E[\tilde{z}_k^j | \mathbf{b}_{0:k-1}^{q \neq i}, \mathbf{b}_k^{m \neq i}, \mathbf{z}_{0:k-1}^i, b_k^j] \right) \quad (27)$$

Substituting (27) in (26) and proceeding by first evaluating the inner expectation, followed by the outer expectation in (26), we obtain the covariance update equation in (6). Due to space constraints, the details are presented in [20].

REFERENCES

- [1] T. Bailey, M. Bryson, H. Mu, J. Vial, L. McCalman, and H. Durrant-Whyte, "Decentralised cooperative localisation for heterogeneous teams of mobile robots," in *In Proc. of the IEEE International Conference on Robotics and Automation*, Shanghai, China, May 9–13, 2011, pp. 2859–2865.
- [2] S. I. Roumeliotis and G. A. Bekey, "Distributed multirobot localization," *IEEE Transactions on Robotics and Automation*, vol. 18, no. 5, pp. 781–795, Oct. 2002.

- [3] A. I. Mourikis and S. I. Roumeliotis, "Optimal sensor scheduling for resource-constrained localization of mobile robot formations," *IEEE Transactions on Robotics*, vol. 22, no. 5, pp. 917–931, Oct. 2006.
- [4] V. Caglioti, A. Citterio, and A. Fossati, "Cooperative, distributed localization in multi-robot systems: A minimum-entropy approach," in *Proc. of IEEE Workshop on Distributed Intelligent Systems: Collective Intelligence and Its Applications*, Prague, Czech Republic, Jun. 15–16, 2006, pp. 25–30.
- [5] E. D. Nerurkar and S. I. Roumeliotis, "Asynchronous multi-centralized cooperative localization," in *Proc. of the IEEE/RSJ International Conference on Intelligent Robots and Systems*, Taipei, Taiwan, Oct. 18–22, 2010, pp. 4352–4359.
- [6] A. Howard, M. J. Mataric, and G. S. Sukhatme, "Localization for mobile robot teams: A distributed MLE approach," in *Experimental Robotics VIII*, 2003, vol. 5, pp. 146–155.
- [7] E. D. Nerurkar, S. I. Roumeliotis, and A. Martinelli, "Distributed Maximum A Posteriori estimation for multi-robot cooperative localization," in *Proc. of the IEEE International Conference on Robotics and Automation*, Kobe, Japan, May 12–17, 2009, pp. 1402–1409.
- [8] A. Ribeiro and G. Giannakis, "Bandwidth-constrained distributed estimation for wireless sensor networks-part I: Gaussian case," *IEEE Transactions on Signal Processing*, vol. 54, no. 3, pp. 1131–1143, Mar. 2006.
- [9] Z.-Q. Luo, "An isotropic universal decentralized estimation scheme for a bandwidth constrained ad hoc sensor network," *IEEE Journal on Selected Areas in Communications*, vol. 23, no. 4, pp. 735–744, Apr. 2005.
- [10] H. C. Papadopoulos, G. W. Wornell, and A. V. Oppenheim, "Sequential signal encoding from noisy measurements using quantizers with dynamic bias control," *IEEE Transactions on Information Theory*, vol. 47, no. 3, pp. 978–1002, Mar. 2001.
- [11] F. A. Shah, A. Ribeiro, and G. B. Giannakis, "Bandwidth-constrained MAP estimation for wireless sensor networks," in *Proc. of 39th Asilomar Conference on Signals, Systems and Computers*, Pacific Grove, CA, Oct. 28–Nov. 1, 2005, pp. 215–219.
- [12] W.-M. Lam and A. R. Reibman, "Design of quantizers for decentralized estimation systems," *IEEE Transactions on Communications*, vol. 41, no. 11, pp. 1602–1605, Nov. 1993.
- [13] J. Gubner, "Distributed estimation and quantization," *IEEE Transactions on Information Theory*, vol. 39, no. 4, pp. 1456–1459, Jul. 1993.
- [14] A. Ribeiro, G. B. Giannakis, and S. I. Roumeliotis, "SOI-KF: Distributed kalman filtering with low-cost communications using the sign of innovations," *IEEE Transactions on Signal Processing*, vol. 54, no. 12, pp. 4782–4795, Dec. 2006.
- [15] P. S. Maybeck, *Stochastic Models, Estimation, and Control*. New York: Academic Press, 1979, vol. 1.
- [16] E. J. Msechu, S. I. Roumeliotis, A. Ribeiro, and G. B. Giannakis, "Decentralized quantized kalman filtering with scalable communication cost," *IEEE Transactions on Signal Processing*, vol. 56, no. 8, pp. 3727–3741, Aug. 2008.
- [17] N. Trawny, S. I. Roumeliotis, and G. B. Giannakis, "Cooperative multi-robot localization under communication constraints," in *Proc. of the IEEE International Conference on Robotics and Automation*, Kobe, Japan, May 12–17, 2009, pp. 4394–4400.
- [18] E. D. Nerurkar, K. X. Zhou, and S. I. Roumeliotis, "A hybrid estimation framework for cooperative localization under communication constraints," in *Proc. of the IEEE/RSJ International Conference on Intelligent Robots and Systems*, San Francisco, CA, Sep. 25–30, 2011, pp. 502–509.
- [19] Y. Bar-Shalom and X.-R. Li, *Estimation and Tracking: Principles, techniques and software*. Norwood, MA: Artech House, Inc., 1993.
- [20] E. D. Nerurkar and S. I. Roumeliotis, "Resource-aware hybrid estimation framework for multi-robot cooperative localization," Dept. of Comp. Sci. & Eng., University of Minnesota, Tech. Rep., 2012, [Online] Available: http://www-users.cs.umn.edu/~nerurkar/Nerurkar_multibithybridCL.pdf.
- [21] S. Lloyd, "Least squares quantization in pcm," *IEEE Transactions on Information Theory*, vol. 28, no. 2, pp. 129–137, Mar. 1982.
- [22] J. Max, "Quantizing for minimum distortion," *IRE Transactions on Information Theory*, vol. 6, no. 1, pp. 7–12, Mar. 1960.
- [23] A. Papoulis, *Probability, random variables, and stochastic processes*, 3rd ed. McGraw-Hill, New York, 1991.